Delft University of Technology

Foot-operated Tele-impedance Interface for Robot Manipulation Tasks in Interaction with Unpredictable Environments

Klevering, S.; Mugge, W.; Abbink, D. A.; Peternel, L.

Citation (APA)
Klevering, S., Mugge, W., Abbink, D. A., & Peternel, L. (2022). Foot-operated Tele-impedance Interface for Robot Manipulation Tasks in Interaction with Unpredictable Environments. In *Proceedings 2022 IEEE/RSJ International Conference on Intelligent Robots and Systems (IROS)* (pp. 3497-3504). IEEE. https://doi.org/10.1109/IROS47612.2022.9981065

Important note
To cite this publication, please use the final published version (if applicable).
Please check the document version above.

Foot-operated Tele-impedance Interface for Robot Manipulation Tasks in Interaction with Unpredictable Environments

Stijn Klevering, Winfred Mugge, David A. Abbink, and Luka Peternel*

Abstract— Tele-impedance increases interaction performance between a robotic tool and unstructured/unpredictable environments during teleoperation. However, the existing tele-impedance interfaces have several ongoing issues, such as long calibration times and various obstructions for the human operator. In addition, they are all designed to be controlled by the operator's arms, which can cause difficulties when both arms are used, as in bi-manual teleoperation. To resolve these issues, we designed a novel foot-based tele-impedance control method inspired by the human limb stiffness ellipse modulation. The proposed mechanical interface design includes a disc and a foot pressure sensor that controls the orientation and size/shape of the stiffness ellipse, respectively. We evaluated the disc interface control method in an experimental study with 12 participants, who performed a complex drilling task in a virtual environment. The results show the ability of the operator to use the proposed interface in order to dynamically adapt to different phases of the task and changes in the environment. In addition, a comparison with low and high uniform impedance modes demonstrates a superior interaction performance of the proposed method.

I. Introduction

Teleoperation is a technology that offers the human operator to remotely control a robot by means of various interfaces. Successful task execution often demands the remote robot to be in physical contact with an unstructured environment, where events are not fully predictable. A classic teleoperation setup that can only command the position of the remote manipulator makes it hard to control the interaction forces, which can result in damaging the environment, manipulator or tool. A solution to increase interaction performance between tool and environment is the inclusion of force feedback to convey proprioceptive or haptic feedback of the manipulator and interaction with the remote environment, which greatly increases telepresence but can be detrimental to stability in some cases [1].

Another solution to increase interaction performance between tool and environment is a control architecture called tele-impedance [1]–[3]. In tasks where a position reference must be tracked, humans tend to increase arm impedance to impose a desired posture/movement by reducing the impact of perturbations [4], [5]. On the other hand, humans decrease the impedance of their limbs to accurately control reference forces during tasks where a force reference must be maintained [6]. Consequently, tele-impedance has the ability to increase the performance of position and force control and compensate for unpredictable perturbations depending

The authors are with Cognitive Robotics and Biomechanical Engineering departments, Delft University of Technology, Delft, The Netherlands.
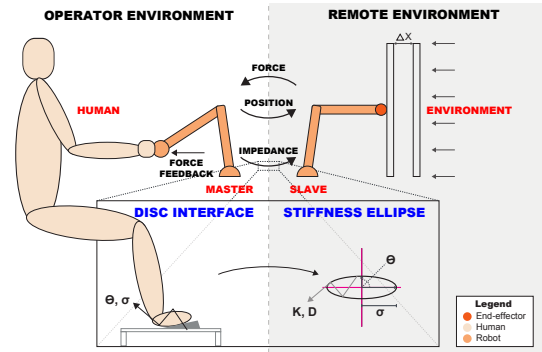*Corresponding author (e-mail: l.peternel@tudelft.nl).

Fig. 1. Bilateral tele-impedance with the proposed foot-operated interface. The human operator controls the motion of the remote robot (slave) with a hand-operated haptic interface (master) and feels force feedback. The operator simultaneously controls the remote robot's stiffness ellipse through the disc interface using a foot. The shape of the stiffness ellipse is defined by orientation θ and principal axes σ that determine how stiff the robot end-effector is in the respective direction of Cartesian space.

on task execution [2], [3]. Classic tele-impedance gives the operator the ability to dynamically change the impedance of the manipulator by replicating the human capacity to adapt endpoint limb impedance [2]. For this, an extra interface is required that enables the human operator to command remote robot stiffness. Characteristic applications of tele-impedance include: assembly [1], human-robot co-manipulation [7], and control of prosthetic hands [8].

Many tele-impedance methods use electromyography-based (EMG) interfaces, which can estimate the stiffness of the operator's arm by measuring muscle activation [2], [7], [9]. These interfaces can be enhanced with human arm posture measurement methods to improve the stiffness estimation [10]. EMG-based interfaces have the ability to generate multi-dimensional variable impedance commands for the remote robot. However, generally, they create an obstruction for the operator due to long calibration times and require additional hardware to be attached to the arm. Furthermore, in bilateral tele-impedance, the force feedback can induce unintended changes to muscle activity and thus the commanded stiffness [11].

Another method is based on estimating the impedance of the operator arm endpoint by inducing force perturbations and measuring corresponding displacements at the haptic device [12]. While this method is effective, perturbing the operator is not always possible due to task requirements or safety (e.g., as in surgery). Furthermore, force feedback from the remote robot can corrupt the measurement. There is also an option to have a shared control system, where the remote robot uses its vision to detect the material of the object with

which the operator intends to interact in order to set a suitable impedance [13]. However, this takes away the control of the impedance from the operator.

It is also possible to command the variable impedance to the remote robot by external devices, such as grip force measurements [3], push-buttons [1] or tablets [14]. External devices are not subject to long calibration times or complicated wearable hardware, however, they often enable commanding impedance only in one dimension at a time. Furthermore, since they are held by the operator's hand, they are hard to apply for bi-manual teleoperation use-cases.

To resolve the issues of the existing stiffness command interfaces in tele-impedance, namely long calibration times, obstruction for the operator with wearable hardware, and occupying hands in case of bi-manual teleoperation, we propose a novel tele-impedance stiffness command interface that is operated with the foot rather than the arm/hand. The *disc interface* design involves a rotating disc to command the stiffness ellipse orientation and a force-sensorised pedal to command its size/shape. For example, rotating the disc with a foot in a certain direction rotates the commanded stiffness ellipse in the same direction, while pressing on the pedal increases the size of the major axis of the ellipse with respect to the minor axis (see Fig. 1 and Fig. 2).

While there are no existing foot interfaces for tele-impedance, there are some for general teleoperation. The state-of-the-art gaming and simulator platforms for driving and flying tend to be based on multiple one degree-of-freedom (DoF) spring-return foot pedals [15]. Some existing surgical systems rely on similar pedals as well [16]. While these offer simplicity, multiple pedals are required for controlling multiple DoF (or variables). Unlike multiple pedals that occupy both feet for operating one device, the proposed interface requires only one foot per device, thus simultaneous bi-manual teleoperation is feasible. It can also be difficult to control all DoF at the same time with multiple pedals [17]. Other teleoperation-specific interfaces track the motion/rotation of the foot either by sensors, such as motion capture systems [18] and inertial measurement units [19], or by mechanical devices [17], [20]–[22]. Nevertheless, in both cases, the movement is limited by the range of the ankle joint [15], which presents another form of obstruction to the operator. Furthermore, they are designed to command the motion/orientation of the remote robot, and not impedance.

Unlike the above-mentioned state-of-the-art foot interfaces, one can rotate the proposed foot interface beyond the range of motion of the ankle. Furthermore, since the commanded rotation depends on the rotation of the disc rather than on the configuration of the foot itself, the operator can keep the foot in a comfortable posture of the ankle in any commanded rotation. Thus, there is no similar design yet for teleoperation in general. Importantly, none of the existing foot interfaces for teleoperation was designed or tested for tele-impedance. In this respect, the proposed interface is unique in enabling the human operator to command the remote robot impedance with the foot. In summary, the main contributions of this paper are: 1) first foot-operated interface

designed specifically for tele-impedance, 2) foot interface whose commands are not limited by the posture of the foot, 3) tele-impedance specific evaluation of the proposed interface in a user study.

Based on the literature and the proposed interface design we test the following design objectives:

- *O1*: The disc interface tele-impedance control method has a superior performance regarding force and position tracking in a dual task in comparison with uniform impedance for unilateral and bilateral control settings.
- *O2*: The disc interface tele-impedance control method has the ability to dynamically change the variable stiffness according to task instruction and situation.
- *O3*: The disc interface introduces no significant increased overall effort of the operator compared to preset uniform impedance modes.

To demonstrate the new design and test the hypotheses we conduct human factor experiments, where participants perform a drilling task while being exposed to force and position perturbations. To evaluate the effect of the bilateral and unilateral control architecture, the experiments are performed under two teleoperation settings: with and without force feedback on a haptic device (Force Dimension Sigma7). To evaluate the performance of the proposed method regarding the interaction with the environment, three conditions are evaluated: high uniform impedance, low uniform impedance and variable impedance controlled by the disc interface. Furthermore, we rotate the environment to alter the required ideal strategy in terms of stiffness ellipse orientation. Finally, we also test the proposed method with respect to the uniform impedance strategies by a NASA Task Load Index (NASA-TLX) subjective analysis to assess the overall workload during the drilling task.

II. Method Overview

The study developed and analysed a novel tele-impedance control method for teleoperation in both unilateral and bilateral teleoperation settings (Fig. 1). The unilateral setting involves no force feedback at the hand-held haptic device, while the bilateral setting includes force feedback from the remote environment. Since we were only interested in the performance regarding position and force tracking during perturbations and not the corrupting effects of real-world bilateral teleoperation issues such as stability, time delay and transparency, we used a virtual impedance-controlled robotic manipulator and a virtual remote environment [11]. Both were generated on the same computer. Furthermore, we assumed that the robotic manipulator was perfectly gravity and inertia compensated. The experiments were conducted on a real hardware setup using the developed disc interface (Fig. 2) and Sigma7 haptic interface (Fig. 3) to perform a drilling task, involving two translations and one orientation.

A. Tele-impedance control

The study involved both bilateral and unilateral tele-impedance controlled methods illustrated in Fig. 1. The
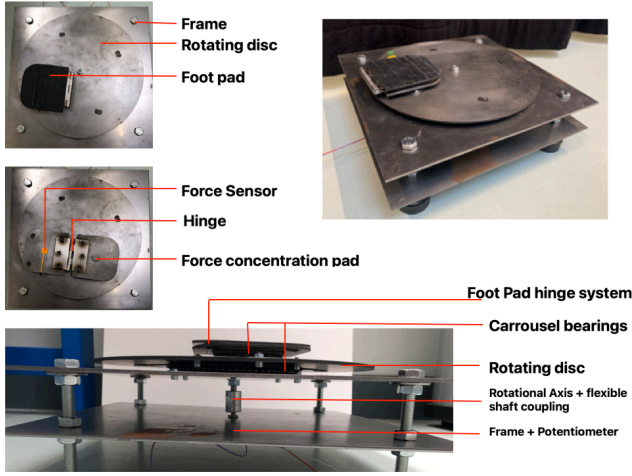
Fig. 2. An overview of the disc interface design. The top left corner shows the top view of the device with the hinged pad closed. The middle photo on the left shows the top view of the device with the hinged pad open to show the force sensor and force concentration pad. The bottom photo shows a side view of the device to indicate the positions of the carousel bearings, rotational axis and flexible shaft coupling with the potentiometer attached under the frame to the rotational axis.

human operator controlled the reference position and a two-dimensional stiffness ellipse located at the end-effector of the remote virtual slave through the disc interface controlled by the foot. The interaction force at the remote site depends on the impedance parameters and the difference between the reference position and velocity (desired position) and the actual position and velocity of the slave as

$$\boldsymbol{f}_{ext} = \boldsymbol{K}(\boldsymbol{x}_d - \boldsymbol{x}_a) + \boldsymbol{D}(\dot{\boldsymbol{x}}_d - \dot{\boldsymbol{x}}_a), \qquad (1)$$

where $\boldsymbol{f}_{ext} \in \mathbb{R}^3$ is the external force acting from the remote robot on the remote environment. Vector $\boldsymbol{x}_a \in \mathbb{R}^3$ is the actual position of the robotic manipulator end-effector and vector $\boldsymbol{x}_d \in \mathbb{R}^3$ is the desired end-effector position controlled by the master. $\boldsymbol{K} \in \mathbb{R}^{3\times3}$ and $\boldsymbol{D} \in \mathbb{R}^{3\times3}$ are the commanded stiffness and damping matrices. The damping matrix was defined as $\boldsymbol{D} = 2\zeta\sqrt{\boldsymbol{K}}$ with $\zeta = 0.7$ to make the system critically damped.

III. INTERFACE DESIGN

We designed a novel foot-operated disc interface that has two inputs; a rotating part that enables rotating a stiffness ellipse and a foot pad that enables elongation of the stiffness ellipse (see Fig. 2). This gives the operator the ability to adjust the stiffness ellipse in a 2D plane in real-time.

A. Design requirements

To support the demands for a successful tele-impedance interface design, the following requirements have to be met:

- *R1*: The operator's arm must not be obstructed by the stiffness command interface.
- *R2*: The interface enables stiffness commands in more than one DoF.
- *R3*: The design does not involve long calibration procedures and knowledge of human anatomy (e.g., for placing muscle electrodes).

- *R4*: The design does not introduce the coupling effect between force-feedback and commanded stiffness [11].

Force-grip [3] and push-button interfaces [1] fail to meet *R1* and *R2*, because of the need for an additional hand-held device to regulate the impedance of the manipulator only in one dimension. Perturbation-based method [12] may interrupt and hinder the operator during the task performance and thus also fails to meet *R1*. The likelihood that an operator will use a tele-impedance device depends on the level that the system will support or hinder their work [23]. Therefore, the system design should minimise calibration times and additional hardware attached to the operator is undesirable. EMG-based interfaces [2] fail to meet *R3* and *R4*, because of the use of EMG interfaces, which involve long calibration procedures and knowledge of the human anatomy to correctly place electrodes on specific muscles. Furthermore, the use of EMG interfaces introduces a coupling effect between the force-feedback and the commanded stiffness that can corrupt the desired commanded stiffness [11].

B. Tele-impedance interface design

Using the Singular Value Decomposition, we are able to generate a stiffness ellipse by two inputs as

$$\boldsymbol{K}_{disc} = \boldsymbol{U}\boldsymbol{E}\boldsymbol{U}^T, \qquad (2)$$

where $\boldsymbol{K}_{disc} \in \mathbb{R}^{2\times2}$ is the stiffness matrix. Note that the existing disc interface design is limited to operating in 2D plane, thus only two DoF of $\boldsymbol{K}$ from (1) can be commanded at a given time. For this study, we limited the experiment task to the horizontal plane, however, an extension to 3D space would be possible by switching between the planes. $\boldsymbol{U} = \begin{bmatrix} cos(\theta) & -sin(\theta) \\ sin(\theta) & cos(\theta) \end{bmatrix}$ is the matrix representing the rotation of the ellipse by Euler angles, where $\theta \in \mathbb{R}^1$ is the rotation angle of the ellipse. $\boldsymbol{E} = \begin{bmatrix} \sigma_1 & 0 \\ 0 & \sigma_2 \end{bmatrix}$ represents the scaling of the stiffness ellipse, where $\sigma_1 \in \mathbb{R}^1$ is the scaling of the major axis and $\sigma_2 \in \mathbb{R}^1$ the scaling of the minor axis. To control the stiffness ellipse with minimum input, the disc interface controls θ and σ_1, while σ_2 is dependent on σ_1.

The disc is connected to a potentiometer that measures the rotation, which is used to control the ellipse orientation shown in Fig. 2. The rotation of the disc has a linear relationship with the rotation of the ellipse. Furthermore, a force sensor is attached under the foot pad using a hinge system to exert the force on the force sensor, which is used to control the major axis of the stiffness ellipse. The control of rotation and shape is applied in the global frame. Therefore, a rotation of the end-effector of the manipulator does not rotate the stiffness ellipse. An important advantage of this is that the human has preoperative feedback about the ellipse orientation, therefore it can infer the state of orientation even without extra visualisation interfaces.

The rotational potentiometer mounted under the structure is attached to a shaft (Fig. 2). We use a flexible shaft coupler to compensate for misalignment. The disc that rotates around the shaft is stabilised by a carousel bearing and the main

3499

frame. To control the rotation of the disc, a foot pad is attached to the disc by a carousel bearing in order to enable a stable movement of the foot in a comfortable posture, while rotating the disc. The rotation of the disc has a linear relationship with the rotation of the ellipse. In our case we used one-to-one scaling, however, other scaling factors can be used. The rotation of the stiffness ellipse is calculated as

$$\theta = \frac{V_\theta}{V_{\theta,max} - V_{\theta,min}}(\theta_{max} - \theta_{min}) + \theta_c, \qquad (3)$$

with the rotation of the stiffness ellipse as $\theta \in \mathbb{R}^1$ and $V_\theta \in \mathbb{R}^1$ as the voltage output of the potentiometer. $V_{\theta,min} \in \mathbb{R}^1$ and $V_{\theta,max} \in \mathbb{R}^1$ are the minimum and maximum voltage output. $\theta_{max} \in \mathbb{R}^1$ and $\theta_{min} \in \mathbb{R}^1$ are the maximum and minimum rotation of the stiffness ellipse and $\theta_c \in \mathbb{R}^1$ is a rotational correction to align the disc interface to the virtual stiffness ellipse. V_θ comes from the rotation of the disc as measured by the potentiometer, while the physical range limits of the potentiometer were between $\theta_{min} = -160°$ and $\theta_{max} = 160°$ (see Fig. 2)

Changing the shape of the ellipse is done by elongating the major axis controlled by a SingleTact force sensor (15mm, 450N/100lb) under the foot pad (see Fig. 2). Force to voltage output has a linear relationship as $V_F = \frac{F_p}{F_{p,max}}(V_{F,max} - V_{F,min})$, where $V_F \in \mathbb{R}^1$ is the voltage output of the force sensor. $F_p \in \mathbb{R}^1$ is the force applied on the footpad by the operator and $F_{p,max} \in \mathbb{R}^1$ the maximum force defined by the force sensor. $V_{F,min} \in \mathbb{R}^1$ and $V_{F,max} \in \mathbb{R}^1$ are the maximum and minimum voltage output. Since the sensor is essentially a variable capacitor that cannot have zero capacitance, exerting zero force has a voltage offset that we need to account for. Therefore, the force sensor has a voltage output translated to major axis scaling $\sigma_1 \in \mathbb{R}^1$ by

$$\sigma_1 = \frac{V_F - V_{F,min}}{V_{F,max} - V_{F,min}}(\sigma_{1,max} - \sigma_{1,min}) + \sigma_{1,min}, \quad (4)$$

where $\sigma_{1,max} \in \mathbb{R}^1$ and $\sigma_{1,min} \in \mathbb{R}^1$ are the maximum and minimum controllable stiffness.

IV. EXPERIMENT METHODS

Twelve male participants between 21 and 36 years old (M = 24.8, SD = 4.0) participated in the experiment. Their participation was voluntary, and their efforts were not financially compensated. The interface design and experiment protocols were approved by the Human Research Ethics Committee of TU Delft and the research was performed in accordance with relevant guidelines and regulations. All subjects gave written informed consent prior to their participation.

A. Experiment setup

To test the design objectives for the disc interface control method we designed a task that involved drilling a hole into an object. The participants performed the drilling task with two teleoperation settings: unilateral and bilateral control. To assess the performance of the disc interface, we compared three impedance conditions applied to the end-effector of the virtual manipulator: high uniform impedance, low uniform
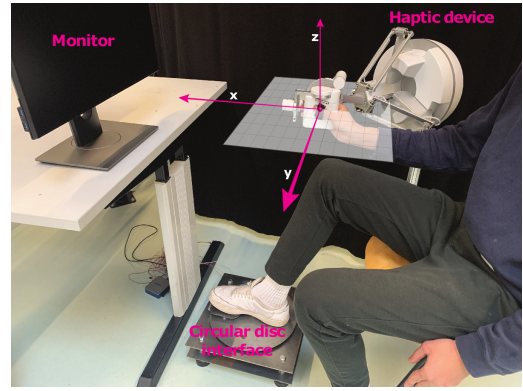

Fig. 3. Illustration of the experiment setup. The participant controlled the Sigma7 haptic device with the right arm and commanded the remote robot stiffness by the disc interface using a foot. The monitor in front of the participant was used to display the remote environment as shown in Fig. 4.

impedance, and variable impedance controlled by the disc interface. The high and low uniform stiffness of the stiffness ellipse located at the end-effector were determined in pilot studies to be 1500 N/m and 200 N/m, respectively. To stimulate the participants to create an ideal stiffness ellipse strategy according to a variable environment, we rotated the environment (-20, -10, 0, 10 and 20°) between sessions.

The experiment setup is shown in Fig. 3. We examined translational movements in the x-axis and y-axis, and rotational movement around the z-axis. A monitor was used to display the drill operated by the remote robot in the virtual environment and a reference force parallel to the insertion direction of the drill in real-time (see Fig. 4). The drilling task consisted of two phases: finding the hole and drill insertion (see Fig. 4).

In the first phase, called the "finding the hole" phase, the participant was instructed to continuously press on the object in the perpendicular direction with 10 N reference force for 10 seconds. On top of that, the participant was instructed to hold the position at the reference position indicated by a red surface area on the object. During the task, the remote robot was subjected to a multi-sine force perturbation perpendicular to the insertion direction. The object indicated that the task was completed by changing color from green to red. Subsequently, the participant had to move the master back to a position located at the negative x-axis of the master to activate the second phase. The ideal strategy for this phase was to be stiff along the direction of perturbation in order to maintain the position on the object [4], [5]. In the direction perpendicular to the object, the stiffness should be low in order to minimise the impact force with the environment [2], [3].

For the second phase called the "drill insertion" phase, the participant had to drill a hole in the object. Like the "finding the hole" phase, the position of drill insertion was indicated by a red surface area on the object. The participant had to maintain the optimal drilling force of 10 N in the insertion direction and was instructed to minimise forces perpendicular to the drilling direction, which could potentially damage the drill or object. During the drilling, the object was subjected
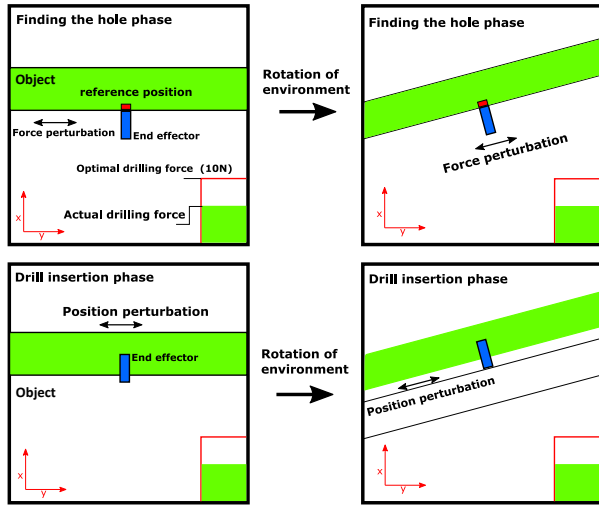
Fig. 4. Unpredictable virtual environment with an object (green), a drill (blue) and the goal position where the hole should be made (red). The actual drilling force with respect to the desired one is displayed by the bar in the bottom right corner. The top two pictures show the "finding the hole" phase with force perturbation direction (e.g., external collisions, wind, water current, etc.). The bottom two pictures show the "drill insertion" phase with positional perturbation direction onto the object (e.g., emulating an unexpected movement of the object or robot). The right column pictures show cases when the object is rotated with respect to the robot base frame.

to a multi-sine position perturbation perpendicular to the insertion direction. The object was infinitely stiff, thus the stiffness of the remote robot had the dominant effect on the interaction force. The ideal strategy for this phase was to be compliant along the direction of perturbation to comply with the movement of the environment (i.e., constraint) and reduce the interaction force between the drill and the object [1]. In the insertion direction, the stiffness should be low in order to maximise the resolution of force control with respect to the difference between the reference and actual positions [1].

B. Experiment protocol

Before the experiment, the participants were familiarised with teleoperation and the stiffness commanding methods. First, a familiarisation session was performed to get acquainted with the environment with and without force feedback by performing the drilling task without perturbations under high and low stiffness conditions. Thereafter, the stiffness ellipse control was introduced and explained. After a thorough explanation of the variable stiffness ellipse, the participants performed the drilling task, including the variable stiffness ellipse control with the disc interface, with and without perturbations. Initially, the participants did it with high and with low uniform impedance, which demonstrated the benefits and drawbacks of both methods. Subsequently, a training session was performed to minimise the effects of learning. One training trial was performed for every impedance condition and force feedback setting during the training phase, resulting in six training trials. The training trials were similar to the experiment trials, with random orientation of the environment.

The experiment sessions involved two force feedback settings (unilateral and bilateral settings) and three impedance

conditions (high uniform impedance, low uniform impedance and variable impedance). During each combination of setting and condition, five rotations of the object (-20, -10, 0, 10, 20°) were used. Therefore, the experiment sessions consisted of 2 settings, 3 conditions and 5 rotations, resulting in a total of 30 trials per participant. To diminish learning effects, we randomised the order of settings, conditions and the rotations of the object among participants based on Latin Square.

C. Dependent measures

During the "finding the hole" task, we analysed the primary (position perpendicular to insertion direction) and secondary (force in insertion direction) task performance. During the insertion task we looked at the primary (force perpendicular to insertion direction) and secondary (force in insertion direction) task performance. In each case, we looked at the subjective results from the NASA-TLX form.

In a drilling task, there is a high probability to damage the tool or environment with high force peaks. Therefore, we used the root mean square error of the force to have more weighting on force peaks.

Finding the hole phase: We quantified task performance as the average of the mean of the absolute error between the signal and a reference position or force. In the following definitions, err and ref are error and reference, respectively, while N is the length of the corresponding time-vector. For the "finding the hole" phase we used the following metrics: *mean absolute position error*: $\bar{\boldsymbol{y}}_{err} = \frac{\sum |\boldsymbol{x}_a - \boldsymbol{x}_{ref}|}{N}$, *root mean square force error*: $\bar{\boldsymbol{F}}_{err} = \frac{\sqrt{\sum (\boldsymbol{F}_a - \boldsymbol{F}_{ref})^2}}{N}$.

Insertion phase: During the insertion phase the following metric was used for both force in insertion direction and perpendicular to insertion direction: *RMSE of force*: $\bar{\boldsymbol{F}}_{err} = \sqrt{\frac{\sum (\boldsymbol{F}_a - \boldsymbol{F}_{ref})^2}{N}}$

Subjective analysis: A NASA-TLX form had to be filled in by the participant between the sessions. In total, we have collected six TLX forms for every control setting and condition per participant.

D. Statistical Analysis

An N-way ANOVA was conducted to compare the position and force errors in different directions between teleoperation control methods, impedance modes and rotations of the environment for both task phases. A significance level of $p \leq 0.05$ is considered a significant difference. Because we are performing multiple analyses on the dataset corresponding to force and position tasks, we use a Bonferroni correction, which compensated for the increased chance of committing a Type 1 error. Afterwards, we conducted a t-test on significant results to compensate for the increased chance of committing a Type 2 error due to the multiple comparisons with Bonferroni correction.

V. RESULTS

A. Finding the hole phase

An N-way ANOVA was conducted to compare the mean absolute position error and root mean square error of interaction force between teleoperation control methods, impedance

	Position error			Force error		
Source	d.f.	F	p	d.f.	F	p
IMP	2	799.12	<0.001	2	37.93	<0.001
FFB	1	746.93	<0.001	1	5.18	0.024
ROT	4	2.73	0.029	4	3.24	0.013
IMP*FFB	2	3.73	0.025	2	1.55	0.214
IMP*ROT	8	0.68	0.071	8	1.73	0.091
FFB*ROT	4	1.16	0.330	4	2.18	0.071
Error	338			338		

[1] In the table, IMP is impedance mode (high uniform, low uniform and variable impedance), FFB is force feedback setting (bilateral and unilateral) and ROT is the rotation of the environment (-20, -10, 0, 10, 20°). The position error is perpendicular to the insertion direction and the force error is parallel to the insertion direction.
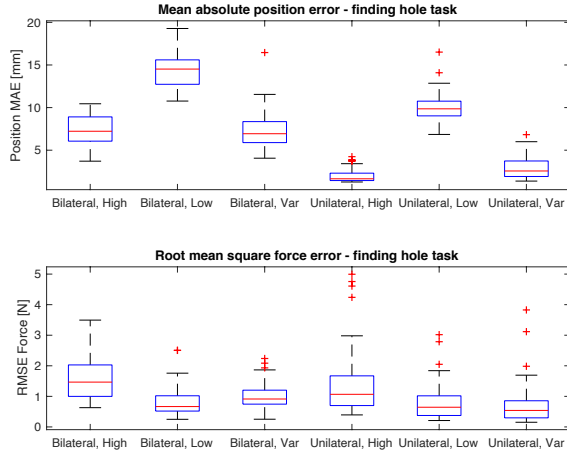
	Perpendicular Force error			Parallel Force error		
Source	d.f.	F	p	d.f.	F	p
IMP	2	407.61	<0.001	2	11.49	<0.001
FFB	1	0.88	0.349	1	0.02	0.875
ROT	4	1.28	0.277	4	0.86	0.490
IMP*FFB	2	2.02	0.134	2	4.60	0.011
IMP*ROT	8	1.82	0.072	8	1.34	0.222
FFB*ROT	4	0.47	0.756	4	1.07	0.371
Error	338			338		

[2] Same description as in Tab. I. The parallel force error is the error considering the optimal drilling reference force of 10N.

Fig. 5. Task performance results for "finding the hole" phase for different force feedback settings and impedance control conditions. The top graph shows the mean absolute position error in the direction perpendicular to the object surface (i.e., along the perturbation) and the bottom graph shows the root mean square of force error in the direction perpendicular to the object (i.e., along the drill). The red line inside the boxplot indicates the median, the box indicates the interquartile range, the arms indicate maximum and minimum data points, while outliers are shown by red crosses.
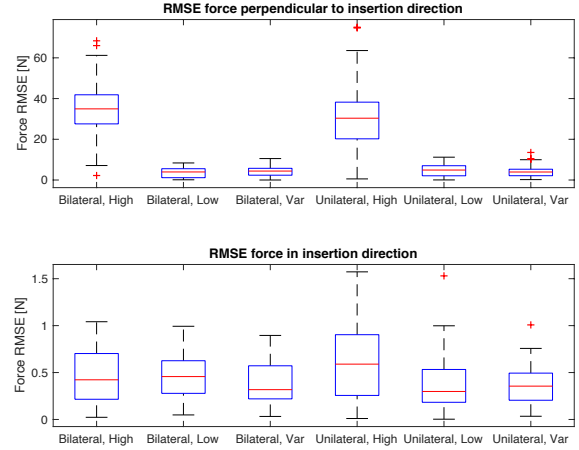

Fig. 6. Task performance results for "drill insertion" phase for different force feedback settings and impedance control conditions. The top graph shows mean root mean square error of force perpendicular to the insertion direction (i.e., along the perturbation) and the bottom graph shows the root mean square of force in the insertion direction (i.e., along the drill). The red line inside the boxplot indicates the median, the box indicates the interquartile range, the arms indicate maximum and minimum data points, while outliers are shown by red crosses.

modes and rotations of the environment. Table I shows the ANOVA results of both dependent measures. The top graph of Fig. 5 shows the absolute position error for the "finding the hole" phase with force feedback setting and impedance mode. The bottom graph of Fig. 5 shows the root mean square error of the interaction force.

The ANOVA on position error perpendicular to insertion direction (i.e., parallel to the object surface) revealed a main effect of impedance mode ($F_{(2,338)} = 799.12$, $p < 0.001$), and a main effect of force feedback setting ($F_{(1,338)} = 746.93$, $p < 0.001$) (Fig. 5 and Tab. I). There was a significant interaction effect between the impedance mode and force feedback setting ($F_{(2,338)} = 3.73$, $p = 0.025$). This means that the effect of impedance mode depends on the effect of the force feedback setting. Post-hoc analysis indicated that the position errors were lower for variable impedance mode than for low uniform impedance mode during both unilateral and bilateral settings ($p < 0.001$). No significant difference was found between high uniform impedance and variable impedance mode during bilateral setting. For the unilateral setting,

a significant larger position error for variable impedance mode in comparison with high impedance mode was found ($p = 0.002$). Furthermore, the effect of force feedback during variable impedance mode yielded a lower position error for the unilateral setting than for the bilateral setting ($p < 0.001$).

The ANOVA on force error parallel to insertion direction (i.e., along the drill) revealed a main effect of impedance mode ($F_{(2,338)} = 37.93$, $p < 0.001$), and a main effect of force feedback setting ($F_{(1,338)} = 5.18$, $p = 0.024$) (Fig. 5 and Tab. I). No significant interaction was found between impedance mode and force feedback setting ($F_{(2,338)} = 1.55$, $p = 0.214$). Post-hoc analysis indicated that the force errors were lower for variable impedance mode than for high impedance mode ($p < 0.001$). Also, larger force errors were found for bilateral teleoperation than for unilateral teleoperation ($p = 0.024$).

B. Drill insertion phase

Table II shows the ANOVA results of both dependent measures. The top graph of Fig. 6 shows the mean squared force error perpendicular to the insertion direction for the "drill insertion" phase for teleoperation setting and impedance
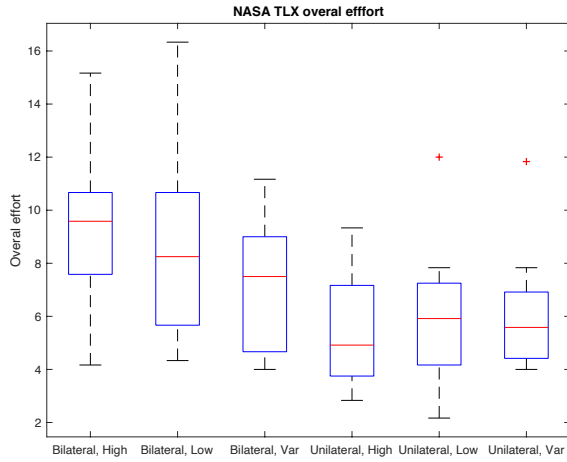
Fig. 7. The overall workload estimated by the RAW NASA-TLX for different impedance modes and force feedback settings.

control. The bottom graph of Fig. 6 shows the root mean square error of the force parallel to the insertion direction.

The ANOVA on force error perpendicular to insertion direction (i.e., parallel to the object surface) revealed a main effect of impedance mode ($F_{(2,338)}=407.61$, $p<0.001$), but no main effect of force feedback setting ($F_{(1,338)}=0.88$, $p=0.349$) (Fig. 6 and Tab. II). No significant interaction was found between impedance mode and force feedback setting ($F_{(2,338)}=2.02$, $p=0.134$). Post-hoc analysis indicated that the force errors were lower for variable impedance mode than for high uniform impedance mode during both force feedback settings ($p<0.001$). No significant difference was found between low uniform impedance and variable impedance modes.

The ANOVA on force error parallel to insertion direction (i.e., along the drill) revealed a main effect of impedance mode ($F_{(2,338)}=11.49$, $p<0.001$), but no main effect of force feedback setting ($F_{(1,338)}=0.02$, $p=0.875$) (Fig. 6 and Tab. II). There was a significant interaction effect between impedance mode and force feedback setting ($F_{(2,338)}=4.60$, $p=0.011$). Post-hoc analysis indicated that the force errors were significantly lower for variable impedance mode than for high uniform impedance mode during unilateral setting ($p<0.001$). No significant difference was found between high uniform impedance and variable impedance modes during the bilateral setting. No significant differences were found between low uniform impedance and variable impedance modes for both force feedback settings.

C. Subjective analysis

Fig. 7 shows the overall workload of the raw NASA-TLX between teleoperation settings and impedance conditions. The ANOVA results of the NASA-TLX questionnaire show a main effect between force feedback settings on overall workload ($F_{(1,66)}=16.42$, $p<0.001$). No interaction between impedance mode and force feedback setting was found. Post-hoc analysis indicated that the overall workload was higher for the bilateral setting than for the unilateral setting ($p<0.001$). Furthermore, no significant main

effect of impedance modes on overall workload was found ($F_{(2,66)}=0.64$, $p=0.529$).

VI. DISCUSSION

1) Design Results: The study introduced a novel tele-impedance interface design for teleoperation applications, called the disc interface, which is controlled with the foot. This can be useful for bi-manual teleoperation due to a free secondary hand, as opposed to some existing stiffness-command interfaces that can occupy both hands for controlling a single remote robotic arm [1], [3], [14]. Hence, the proposed interface meets the requirements *R1* and *R4*, in contrast to the hand-held tele-impedance devices [1], [3], [14] that do not. Since the interface can modulate the stiffness ellipse by two independent inputs, it fulfils requirement *R2*.

Tele-impedance methods using EMG and positional measurements enable a multi-dimension variable impedance [2], [10]. However, these methods generally require long equipping and calibration times, additional knowledge of human anatomy, and additional hardware, such as EMG sensors and motion capture markers. This adds up to a decrease in the probability of utilisation and comfort of the operator [23]. In contrast, the disc interface is not a wearable device and only requires calibration for rotational precision. Thus, it meets requirements *R1* and *R3*, respectively.

The tele-impedance control method was evaluated during uni-manual teleoperation but has the capacity to be used for bi-manual teleoperation, due to a free secondary arm and foot. Therefore, we strongly recommend further exploring the influence of the interface design for bi-manual teleoperation regarding position and force tracking performance and workload of the operator. The interface can also be used for altering a stiffness ellipsoid rather than an ellipse, where the interface can change the rotation and shape of the ellipse in multiple 2D planes independently by switching control modes via voice commands [13]. Furthermore, the disc interface can be used for teaching methods [1] involving variable stiffness transfer in multiple DoF.

2) Experiment results: The participants were able to command the rotation of the stiffness ellipse relative to the rotation of the environment in order to achieve an ideal strategy for the task execution and environment. Design objective *O2* was achieved as participants were able to perform position and force tracking tasks in multiple directions by dynamically adapting the stiffness ellipse to a changing environment. In fact, Figs. 5 and 6 show that the ability to adapt the stiffness ellipse improved the task performance compared to constant stiffness settings. This is in line with how the human central nervous system adapts the endpoint stiffness ellipsoid of the arm based on the interaction with unpredictable and unstructured environments [4], [5]. Furthermore, it is consistent with results of dynamic adaptation in other tele-impedance studies [1], [2].

During the "finding the hole" phase for both unilateral and bilateral teleoperation, the disc interface allowed for a significantly improved position tracking compared to low uniform impedance mode, and a significantly improved force

tracking compared to the high uniform impedance mode. This suggests that tele-impedance control increases the interaction performance between tool and environment and improves tracking of a reference position for both teleoperation settings in comparison with uniform impedance, which confirms design objective *O1*.

During the insertion phase, the participants used the disc interface to generate a low uniform impedance required for the force tasks in the parallel and perpendicular insertion direction. Since the end-effector was constrained by the environment, high impedance was not desired [1]. During this phase, both the low uniform impedance and the variable impedance modes performed significantly better regarding force tracking in comparison with the high uniform impedance mode during unilateral teleoperation. There was no significant difference of the force tracking error in insertion direction during bilateral teleoperation. This could be due to the introduction of human arm stiffness dynamics by force feedback [11]. The performance analysis confirmed our design objective *O1*. This is especially true for the "finding the hole" phase but not for the "drill insertion" phase due to a similar performance between low uniform impedance and variable impedance modes. Since drilling tasks consist of two phases, we can confirm that our design objective *O1* is true for the drilling task.

3) Subjective analysis: The subjective analysis by the NASA-TLX did not show a significant statistical difference in overall effort between impedance control conditions, which confirms the design objective *O3*. This can be explained by an increase in effort due to the use of the disc interface but a decrease of effort by an easier task execution due to the introduction of the variable stiffness. Furthermore, participants experienced a statistically significant higher workload during bilateral teleoperation in comparison with unilateral teleoperation. This can be attributed to the force feedback that requires exerting force at the master.

VII. Conclusion

We have developed and experimentally evaluated a novel foot-operated disc interface for tele-impedance. By design, the proposed interface is not restricted by foot range of motion as current foot interfaces for classic teleoperation are. The user study showed that the operator could effectively use it to command various shapes and sizes of stiffness ellipsoid, as required by the tasks in unpredictable environments.

References

[1] L. Peternel, T. Petrič, and J. Babič, "Robotic assembly solution by human-in-the-loop teaching method based on real-time stiffness modulation," *Autonomous Robots*, vol. 42, no. 1, pp. 1–17, 2018.

[2] A. Ajoudani, N. Tsagarakis, and A. Bicchi, "Tele-impedance: Teleoperation with impedance regulation using a body–machine interface," *The International Journal of Robotics Research*, vol. 31, no. 13, pp. 1642–1656, 2012.

[3] D. S. Walker, J. K. Salisbury, and G. Niemeyer, "Demonstrating the benefits of variable impedance to telerobotic task execution," in *2011 IEEE International Conference on Robotics and Automation (ICRA)*, 2011, pp. 1348–1353.

[4] E. Burdet, R. Osu, D. W. Franklin, T. E. Milner, and M. Kawato, "The central nervous system stabilizes unstable dynamics by learning optimal impedance," *Nature*, vol. 414, no. 6862, pp. 446–449, 2001.

[5] A. Naceri, T. Schumacher, Q. Li, S. Calinon, and H. Ritter, "Learning optimal impedance control during complex 3d arm movements," *IEEE Robotics and Automation Letters*, vol. 6, no. 2, pp. 1248–1255, 2021.

[6] W. Mugge, D. A. Abbink, A. C. Schouten, J. P. Dewald, and F. C. Van Der Helm, "A rigorous model of reflex function indicates that position and force feedback are flexibly tuned to position and force tasks," *Exp. brain research*, vol. 200, no. 3, pp. 325–340, 2010.

[7] L. Peternel, N. Tsagarakis, and A. Ajoudani, "A human–robot co-manipulation approach based on human sensorimotor information," *IEEE Transactions on Neural Systems and Rehabilitation Engineering*, vol. 25, no. 7, pp. 811–822, 2017.

[8] A. Ajoudani, S. B. Godfrey, M. Bianchi, M. G. Catalano, G. Grioli, N. Tsagarakis, and A. Bicchi, "Exploring teleimpedance and tactile feedback for intuitive control of the pisa/IIT soft hand," *IEEE Transactions on Haptics*, vol. 7, no. 2, pp. 203–215, 2014.

[9] S. Park and W. K. Chung, "Tele-impedance control of virtual system with visual feedback to verify adaptation of unstable dynamics during reach-to-point tasks," in *2016 IEEE International Conference on Biomedical Robotics and Biomechatronics*, 2016, pp. 1283–1289.

[10] C. Fang, G. Rigano, N. Kashiri, A. Ajoudani, J. Lee, and N. Tsagarakis, "Online joint stiffness transfer from human arm to anthropomorphic arm," in *2018 IEEE International Conference on Systems, Man, and Cybernetics (SMC)*, 2018, pp. 1457–1464.

[11] L. M. Doornebosch, D. A. Abbink, and L. Peternel, "Analysis of coupling effect in human-commanded stiffness during bilateral tele-impedance," *IEEE Transactions on Robotics*, vol. 37, no. 4, pp. 1282–1297, 2021.

[12] G. Gourmelen, B. Navarro, A. Cherubini, and G. Ganesh, "Human guided trajectory and impedance adaptation for tele-operated physical assistance," in *2021 IEEE/RSJ International Conference on Intelligent Robots and Systems (IROS)*, 2021, pp. 9276–9282.

[13] Y.-C. Huang, D. A. Abbink, and L. Peternel, "A semi-autonomous tele-impedance method based on vision and voice interfaces," in *2021 20th International Conference on Advanced Robotics (ICAR)*, 2021, pp. 180–186.

[14] L. Peternel, N. Beckers, and D. A. Abbink, "Independently commanding size, shape and orientation of robot endpoint stiffness in tele-impedance by virtual ellipsoid interface," in *2021 20th International Conference on Advanced Robotics (ICAR)*, 2021, pp. 99–106.

[15] E. Velloso, D. Schmidt, J. Alexander, H. Gellersen, and A. Bulling, "The feet in human–computer interaction: A survey of foot-based interaction," *ACM Computing Surveys*, vol. 48, no. 2, pp. 1–35, 2015.

[16] A. Mirbagheri, F. Farahmand, B. Ghanadi, K. A. Khoiy, S. Porsa, M. J. Shamsollahi, M. H. Owlia, F. Karimian, and K. Toulabi, "Operation and human clinical trials of robolens: an assistant robot for laparoscopic surgery," *Frontiers in Biomedical Technologies*, vol. 2, no. 3, pp. 184–190, 2015.

[17] Y. Huang, W. Lai, L. Cao, E. Burdet, and S. J. Phee, "Design and evaluation of a foot-controlled robotic system for endoscopic surgery," *IEEE Robotics and Automation Letters*, vol. 6, no. 2, pp. 2469–2476, 2021.

[18] E. Abdi, E. Burdet, M. Bouri, and H. Bleuler, "Control of a supernumerary robotic hand by foot: An experimental study in virtual reality," *PloS one*, vol. 10, no. 7, p. e0134501, 2015.

[19] F. Zhong, P. Li, J. Shi, Z. Wang, J. Wu, J. Y. Chan, N. Leung, I. Leung, M. C. Tong, and Y.-H. Liu, "Foot-controlled robot-enabled endoscope manipulator (freedom) for sinus surgery: design, control, and evaluation," *IEEE Transactions on Biomedical Engineering*, vol. 67, no. 6, pp. 1530–1541, 2019.

[20] E. Abdi, M. Bouri, J. Olivier, and H. Bleuler, "Foot-controlled endoscope positioner for laparoscopy: Development of the master and slave interfaces," in *2016 4th International Conference on Robotics and Mechatronics (ICROM)*, 2016, pp. 111–115.

[21] B. W. Rudolph, *Foot-controlled Supernumerary Robotic Arm: Foot Interfaces and Human Abilities*. Rose-Hulman Inst. of Tech., 2019.

[22] W. Amanhoud, J. Hernandez Sanchez, M. Bouri, and A. Billard, "Contact-initiated shared control strategies for four-arm supernumerary manipulation with foot interfaces," *The International Journal of Robotics Research*, vol. 40, no. 8-9, pp. 986–1014, 2021.

[23] D. A. Abbink, T. Carlson, M. Mulder, J. C. de Winter, F. Aminravan, T. L. Gibo, and E. R. Boer, "A topology of shared control systems-finding common ground in diversity," *IEEE Transactions on Human-Machine Systems*, vol. 48, no. 5, pp. 509–525, 2018.